

RSC Advances



This is an *Accepted Manuscript*, which has been through the Royal Society of Chemistry peer review process and has been accepted for publication.

Accepted Manuscripts are published online shortly after acceptance, before technical editing, formatting and proof reading. Using this free service, authors can make their results available to the community, in citable form, before we publish the edited article. This *Accepted Manuscript* will be replaced by the edited, formatted and paginated article as soon as this is available.

You can find more information about *Accepted Manuscripts* in the [Information for Authors](#).

Please note that technical editing may introduce minor changes to the text and/or graphics, which may alter content. The journal's standard [Terms & Conditions](#) and the [Ethical guidelines](#) still apply. In no event shall the Royal Society of Chemistry be held responsible for any errors or omissions in this *Accepted Manuscript* or any consequences arising from the use of any information it contains.

Hierarchical Porous TiO₂ Templated from Natural Artemia Cyst Shells for Photocatalysis Applications

Yufeng Zhao^{1*}, Yunjuan He¹, Jing He¹, Yuqin Ren³, Zhifeng Liu^{2**}, Wenfeng Guo¹, Faming Gao¹

¹Key Laboratory of Applied Chemistry, Department of Environmental and Chemical Engineering, Yanshan University, 066004, Qinhuangdao, China. ²Department of Materials Science and Engineering, Tianjin Chengjian University, 300384, Tianjin, China. ³Beidaihe Center Experiment Station, Chinese Academy of Fishery Science, 066100, Beidaihe, China

Abstract: A novel hierarchical porous TiO₂ is successfully synthesized through a sol-gel method, using a natural cyst shell as hard template. The morphology characterization shows that the as-prepared TiO₂ with a hierarchical porous architecture is assembled by multiple-layered porous nanosheets. The degradation of methylene blue dye in water can rapidly reach 96% with as-prepared TiO₂ after 50 min, showing an improved photocatalytic efficiency of 13% as compared to commercial TiO₂.

Keywords: hierarchical porous; natural template; titanium dioxide; photocatalytic activity

Introduction

Titanium dioxide (TiO₂), a typical semiconductor with wide-band, has been extensively investigated owing to its promising applications in catalysts, photo-splitting of water¹, self-cleaning², gas sensors, and photovoltaic cells³⁻⁹ etc. One of the most important applications of TiO₂ is as a photocatalyst in environmental protection due to its chemical stability, strong oxidation activity, chemical stability, and nontoxicity^{10,11}. In practical application, the photocatalytic performance of TiO₂ is strongly influenced by the crystal structure, morphology, and crystallite size¹²⁻¹⁵. Thus, design and synthesis of nanocrystals with well-defined morphologies is significant in tailoring the properties.

Up to now, various morphologies of TiO₂, such as nanorods¹⁶, nanowires¹⁷, nanotubes^{18,19}, have been successfully developed through different methods. However, the low dimensional nanoscaled building blocks have more chances to aggregate in the process of synthesis and photocatalysis, leading to shrinkage of its specific surface and photocatalytic and photoelectrochemical performance. While three-dimensional (3D) hierarchical structured TiO₂ can avoid this problem. In addition, this kind of materials combines the catalytic properties of smaller pore systems and the available diffusion pathways of macroporous networks with high surface area²⁰⁻²⁵. Tao et al.²⁶ synthesized

*corresponding author, E-mail: yufengzhao@ysu.edu.cn

**corresponding author, E-mail: address: tjulzf@163.com

hierarchical nanostructured TiO₂ spheres via hydrothermal method in NaOH solution. Zhao et al.²⁷ prepared highly oriented hierarchical structured rutile TiO₂ nanoarrays through a hydrothermal method and assembled it to form dye-sensitized solar cells, harvesting a better fill factor and higher conversion efficiency. Liu et al.²⁸ synthesized nanostructured TiO₂ with different hierarchical morphologies via a hydrothermal route by, and their morphology-dependent photocatalytic performance for phenol degradation was evaluated.

In this work, a novel hierarchical porous TiO₂ was synthesized by a facile and low cost sol-gel method, in which a natural material, Artemia cyst shell (AS) was used as hard template, which was reported to possess with a hierarchical porous inner cortical structure²⁹. The photocatalytic activity of the as-prepared TiO₂ was evaluated by degradation methylene blue (MB), showing an improved photocatalytic efficiency of 13% as compared to commercial TiO₂.

Experimental

The hierarchical porous TiO₂ was synthesized in an improved sol-gel approach. Specifically, 5 ml butyl titanate was dissolved in 10 ml anhydrous ethanol at 50 °C, the pH value was adjusted to 2 with concentrated hydrochloric acid. Subsequently a mixture including anhydrous ethanol, glacial acetic acid and deionized water in the proportion of 5:2:1 (v:v:v) was dropped into the above solution slowly. Finally the ball-milled AS was added, the obtained system was drastically stirred for 1 h and kept overnight at room temperature to allow the thorough adsorption of titania sol into the AS structure. The as-prepared product was gently heated in an oven at 80 °C overnight. Finally, hierarchical porous TiO₂ was obtained after the AS template was removed upon subsequent heat treatment at 500 °C for 10 h in air.

Powder X-ray diffraction (XRD) patterns of samples were recorded on a D-max-2500/PC X-ray diffractometer (Japan, Rigaku, Cu K α). The sample morphology was examined in a Hitachi-S4800 field emission scanning electron microscope (FESEM, Japan) and Hitachi-7650 transmission electron microscopy (TEM, Japan). The chemical composition of the product was characterized by EDS (Energy-dispersive X-ray spectroscopy, Horiba, 7539-H). The specific surface area (SSA) and pore size distribution were investigated with nitrogen cryosorption (Micromeritics, ASAP2020).

The photocatalytic properties of hierarchical porous TiO₂ were investigated, by using high pressure xenon lamp as the light source, and MB solution as the degradation target. Prior to illumination, 100 ml of MB aqueous solutions (10 mg/L) containing 0.03 g samples were magnetically stirred in the dark for 30 min to achieve adsorption/desorption equilibrium and better dispersion. During irradiation, a series of samples were taken from the reactor every 10 min and the

degree of MB degradation was determined via UV-Vis. According to the degree of MB degradation, the photocatalytic activity of the as-prepared TiO₂ was evaluated.

Results and Discussion

The XRD pattern of commercial TiO₂ and the as-prepared hierarchical porous TiO₂ is shown in **Figure 1**, which indicates the synthesized sample displays a good crystallinity. The characteristic peaks of tetragonal anatase TiO₂ (JCPDS NO.21-1272, space group 141/amd (141)) were observed. The morphology of the AS template and as-obtained TiO₂ was observed under FESEM and TEM as shown in **Figure 2**. **Figure 2a** and **2b** demonstrate the microstructure of the AS before and after ball milling respectively. The net-like hierarchical porous structure on the AS is fairly exposed after ball-milling, which can be easily duplicated. SEM image of the as-prepared TiO₂ calcined at 500 °C are shown in **Figure 2c**, it indicates that the product shows a net-like 3-D hierarchical porous structure with good connectivity between pore walls. The structure is multi-layered, from which macropores, ranging in diameter mainly from 200 to 700 nm, can be obviously observed. TEM images further proved the hierarchical porous architecture of our obtained TiO₂, as shown in **Figure 2d** and **Figure 2e**, and indicated that the pore wall was assembled by TiO₂ nanoparticles. **Figure 2f** is a typical high-resolution TEM (HRTEM) image on the pore walls, which reveals the presence of many nanocrystals showing anatase lattice fringes, indicating that the wall of the pores is assembled by such TiO₂ nanocrystals, and the average crystallite size is about 5 nm. The interplanar spacing is measured to be 0.35 nm, which is consistent with that of the anatase (101) crystal faces. EDS analysis of the as-prepared TiO₂ indicates the existence of element Fe, S and Ca besides Ti and O (**Figure 3a**), these heteroatoms should be resulted from the natural Artemia cyst shell, which could be self-doped to the hierarchical porous TiO₂.

The nitrogen adsorption-desorption isotherm plot and the corresponding pore-size distribution curve for as-prepared TiO₂ are shown in **Figure 3b**. It reveals that the nitrogen sorption isotherm presents a reverse “S” shape, which is identified as IV-type according to the Brunauer classification³⁰. The BET specific surface area is measured to be 124 m²/g. This value is high enough and comparable to those reported porous TiO₂ from literature^{31, 32}. Barrett-Joyner-Halenda (BJH) analysis (**Figure 3b** inset) reveals that most of the pores fall into the size range of 2-4 nm, suggesting the coexistence of micropores (≤ 2 nm) and mesopores (2~50 nm). Macropores (≥ 50 nm) detected in SEM picture cannot be accurately measured through BJH method. This hierarchical porous structure facilitates the efficient diffusion and transportation of the degradable organic molecules in photochemical reaction, which will contribute to the photocatalytic activity of TiO₂

material³³.

The possible formation mechanism of the hierarchical porous structure can be explained by a surface sol-gel coating process^{34, 35}. At the initial stage of sol-gel synthesis, titanium ion was chemisorbed onto AS surface which is abundant with hydroxylated groups. After the addition of water, Ti(OH)₄ colloids as the precursor of TiO₂ nano-particle in the pore wall formed due to a hydrolysis of Ti(OC₄H₉)₄. During this sol-gel process, anhydrous ethanol was used as solvent, and glacial acetic acid was added dropwisely to adjust the acidity of the reaction system. After further nucleation and growth, the TiO₂ nanocrystals were assembled into hierarchical architectures of AS. And the target sample was obtained after AS template was removed by calcination treatment.

Figure 4 (a) displays the room temperature absorbance spectra of commercial TiO₂ and hierarchical porous TiO₂. The data were recorded in the wavelength range of 200-800 nm and the absorption edges were approximately 380, 480 nm, respectively. It can be seen that the hierarchical porous TiO₂ shows a wide absorbance in the visible region and obvious red shift than that of the commercial TiO₂. The red-shift should be due to the elements doping of Fe and S inherited from the Artemia cyst shell during the material preparation³⁶⁻³⁸. The band gap of TiO₂ can be calculated from the Uv-vis absorbance data, via the equation $\alpha h\nu = k(h\nu - E_g)^m$, where α is the absorption coefficient, E_g is the optical band gap, k is a constant and $m = 1/2$. A typical plot of $(\alpha h\nu)^2$ versus $h\nu$ was plotted using the data obtained from the optical absorption spectra (**Figure 4(b)**). The band gap of the as-prepared hierarchical porous TiO₂ is calculated to be 2.95 eV, showing an obvious decrease compared to the commercial one (3.20 eV).

The photocatalytic activity of the samples was investigated by degrading a common organic dye methylene blue (MB) under weak alkaline condition. **Figure 4 (c)** presents the optical absorption spectra of MB aqueous solution (initial concentration: 10mg/L, 100 mL) with 30 mg of the as-prepared TiO₂ powders after exposure to high pressure mercury lamp for different time. The maximum absorption peak locates at 614 nm, corresponding to the MB molecules. And the absorption peak shrinks gradually with the extension of exposure time, until almost completely disappears after about 50 min. A series of color changes of MB solution during the irradiation are shown in the upper part of the inset photo in **Figure 4 (c)**. Notably, the intense blue color of the starting solution gradually fades with the extension of exposure time, which is corresponding to the sequential changes of the optical absorbance spectra.

The degree of MB degradation versus the exposure time from the optical absorbance measurement at 614 nm are shown in **Figure 4 (d)**. C_0 refers to the initial methylene blue

concentration (after the dark reaction), and C is the concentration of methylene blue samples taken during the photocatalytic experiment. It indicates that the as-prepared TiO₂ shows a high photocatalytic activity, as the degradation of MB can reach 96% at 50 min with the presence of as-prepared hierarchical porous TiO₂ catalyst. As contrast, the photocatalytic activity of commercial TiO₂ is also investigated under the same condition, of which the degradation of MB only reaches 85%. The superior photocatalytic performance of the as-prepared TiO₂ can be ascribed to the special structure features. On one hand, the product has a perfect hierarchical structure, and it possesses a greater accessible specific surface area owing to its open and network structure features, which make the sample have more catalytically active sites. Besides, light would be reflected much more times among the hierarchical porous and the multiple reflections would extend the light propagation path, which is beneficial to the full utilization of incident light and enhance the photocatalytic property. On the other hand, the Fe and S element doping leads to red shift, thus broadens the absorbance range of light, and produces more photoproduction of electron and hole, thus the photocatalytic performance of the as-prepared TiO₂ can be enhanced. Furthermore, the bigger size of the hierarchical porous TiO₂ blocks can effectively prevent the aggregation and help enhance the photocatalytic activity²⁰. A more detailed and deeper investigation of durability of the photocatalytic activity and the structure stability of the hierarchical porous TiO₂ is under progress.

Conclusions

In summary, the natural templating approach has been shown to provide a facile, environmental friendly and biomimetic method for the synthesis of hierarchical porous TiO₂. Owing to its special structure and self-doping of heteroatoms, such TiO₂ presents superior photocatalytic activity as compared to commercial TiO₂. This indicates that the as-prepared hierarchical porous TiO₂ could be a promising candidate for photocatalysis application or waste water treatment, because of the facileness in preparation, reproductivity and recycling.

Acknowledgement

Financial support from the National Natural Science Foundation of China (Grant 51202213), Natural Science Foundation of Hebei Province (Grant B2012203043), China Postdoctoral Science Foundation (Grant 2013M530889), Excellent Young Scientist Funding of Hebei Province (Grant Y2012005) and Postdoctoral Foundation in Hebei Province is acknowledged.

[1] K. Guo, Z. Liu, C. Zhou, J. Han, Y. Zhao, Z. Liu, Y. Li, T. Cui, B. Wang, J. Zhang, *Appl. Catal. B.* 2014, 154-155, 27-35.

[2] Z. Liu, Y. Wang, X. Peng, Y. Li, Z. Liu, C. Liu, J. Ya, Y. Huang, *Sci. Technol. Adv. Mater.* 2012,

13, 025001-025005.

[3] T. L. Thimpson, J. T. Yates, *Chem. Rev.* 2006, 106, 4428-4453.

[4] X. T. Zhang, M. Jin, Z. Y. Liu, S. Nishimoto, H. Saito, T. Murakami, A. Fujishima, *Langmuir* 2006, 22, 9477-9479.

[5] H. X. Li, Z. F. Bian, J. Zhu, D. Q. Zhang, G. S. Li, Y. N. Huo, H. Li, Y. F. Lu, *J. Am. Chem. Soc.* 2007, 129, 8406-8413.

[6] D. Kuang, J. Brillet, P. Chen, M. Takata, S. Uchida, H. Miura, K. Sumioka, S. M. Zakeeruddin, M. Gratzel. *ACS Nano* 2008, 2, 1113-1116.

[7] K. Shankar, J. Bandara, M. Paulose, H. Wietasch, O. K. Varghese, G. K. Mor, T. J. Latempa, M. Thelakkat, C. A. Grimes, *Nano Lett.* 2008, 1654-1659.

[8] Z. Liu, Y. Li, C. Liu, J. Ya, L. E, W. Zhao, D. Zhao, L. An, *ACS Appl. Mater. Interfaces.* 2011, 3, 1721-1725.

[9] C. Liu, Z. Liu, L. E, Y. Li, J. Han, Y. Wang, Z. Liu, J. Ya, X. Chen, *Electron. Mater. Lett.* 2012, 8, 481-484.

[10] C. S. Guo, M. Ge, L. Liu, G. D. Gao, Y. C. Feng, Y. Q. Wang, *Environ. Sci. Technol.* 2010, 44, 419.

[11] L. Q. Jing, H. G. Fu, B. Q. Wang, D. J. Wang, B. F. Xin, S. D. Li, J. Z. Sun, *Appl. Catal. B.* 2006, 629, 282.

[12] N.-G. Park, J. van de Lagemaat, A. J. Frank, *J. Phys. Chem. B.* 2000, 104, 8989-8994.

[13] Y. Fu, Z. Jin, Y. Ni, H. Du, T. Wang, *Thin Solid Films*, 2009, 517, 19, 2009, 5634-5640.

[14] J. Y. Liao, J. W. He, H. Xu, D. B. Kuang, C. Y. Su, *J. Mater. Chem.*, 2012, 22, 7910-7918.

[15] J. G. Yu, J. J. Fan, L. Zhao, *Electrochim. Acta*, 2010, 55, 597-602.

[16] H. M. Cheng, J. M. Ma, L. M. Qi, *Chem. Mater. J.* 1995, 7, 663-671.

[17] Z. Miao, D. S. Xu, J. H. Ouyang, G. L. Guo, X. S. Zhao, Y. Q. Tang, *Nano Lett. J.* 2002, 2, 717-720.

[18] G. Y. Guo, J. S. Hu, H. P. Liang, L. J. Wang, C. L. Bai, *Adv. Fun. Mater. J.* 2005, 15, 196-202.

[19] T. Kasuga, M. Hiramatsu, A. Hoson, T. Sekino, K. Niihara, *Adv. Mater. J.* 1999, 11, 1307-1311.

[20] J. R. Lakowicz, *Principles of Fluorescence Spectroscopy*, Plenum Press, New York 1999.

[21] S. Zhu, D. Zhang, Z. Chen, G. Zhou, H. Jiang, J. Li, *J. Nanopart Res.* 12(7):2445-2456.

[22] C.C. Chau, W. R. Follette, *Adv. Mater.* 2000, 12, 1859-1864.

[23] E. R. Zubarev, M. U. Pralle, E. D. Sone, S. I. Stupp, *J. Am. Chem. Soc.* 2001, 123, 4105.

- [24] A. Chen, J. Qian, C. Yang, X. Lu, F. Wang, Z. Tang, Powder Tech. 2013, 249, 71-76.
- [25] G. Zhu, B. Yang, S. Wang, Int. J. Hydrogen Energ. 2011, 36, 13603-13613.
- [26] J. Tao, J. Deng, X. Dong, H. Zhu, H. J. Tao, Trans. Nonferrous Met. Soc. China, 2012, 22, 2049-2056.
- [27] Y. Zhao, X. L. Sheng, J. Zhai, L. Jiang, C. H. Yang, Z. W. Sun, Y. F. Li, D. B. Zhu, ChemPhysChem, 2007, 8, 856-861.
- [28] L. Liu, H. J. Liu, Y. P. Zhao, Y. Q. Wang, Y. Q. Duan, G. D. Gao, M. Ge, W. Chen, Environ. Sci. Technol. 2008, 42, 2342-2348.
- [29] S. F. Wang, S. C. Sun, Microsc. Res. Tech. 2007, 70, 663-670.
- [30] G.M. Clavier, J.L. Pozzo, H. Bouas-Laurent, C. Liere, C. Roux, C. Sanchez, J. Mater. Chem. 2000, 10, 1725-1730.
- [31] R. A. Caruso, M. Giersig, F. Willig, M. Antonietti, Langmuir 1998,14, 6333-6336.
- [32] R. A. Caruso, J. H. Schattka, Adv. Mater. 2000, 12, 1921-1923.
- [33] B. X. Li, Y. F. Wang, J. Phys. Chem. C 2010, 114, 890-896.
- [34] I. Ichinose, H. Senzu, T. Kunitake, Chem. Lett.1996, 831-832.
- [35] R. A. Caruso, Angew. Chem. Int. Ed. 2004, 43, 2746-2748.
- [36] W. Choi, A. Termin, M.R. Hoffmann, J. Phys. Chem. 1994, 98, 13669-13679
- [37] T. Ohno, M. Akiyoshi, T. Umebayashi, K. Asai, T. Mitsui, M. Matsumura, Appl. Catal. A 2004, 265, 115-121
- [38] M.H. Zhou, J.G. Yu, B. Cheng, H.G. Yu, Mater. Chem. Phys. 93 (2005), 159-163

Figure Captions

Figure 1. XRD patterns of commercial TiO₂ and obtained hierarchical porous TiO₂.

Figure 2. SEM image of (a) Artemia cyst shell, (b) AS debris (after ball milling), (c) the as-prepared hierarchical porous TiO₂; (d) TEM image of the as-prepared hierarchical porous TiO₂; (e) the corresponding local magnification image of (d); (f) the corresponding HRTEM image.

Figure 3. (a) EDS patterns of the as-prepared TiO₂ and template AS (inset); (b) Nitrogen adsorption-desorption isotherms plots and pore size distribution plots of as-prepared TiO₂ (inset).

Figure 4. (a) UV-Visible absorption spectrum; (b) plot of $(ah\nu)^2$ versus $h\nu$ for the TiO₂ samples; (c) Time-dependent color change and corresponding time-dependent absorption spectrum of MB in the presence of as-prepared TiO₂; (d) The degree of MB degradation with catalysts versus the exposure time, where C₀ refers to the initial methylene blue concentration (after the dark reaction).

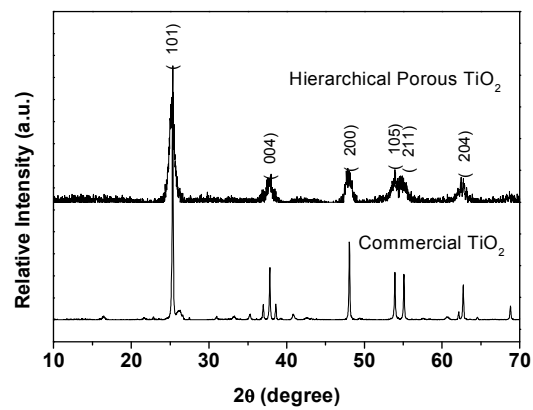


Figure 1. XRD patterns of commercial TiO_2 and obtained hierarchical porous TiO_2 .

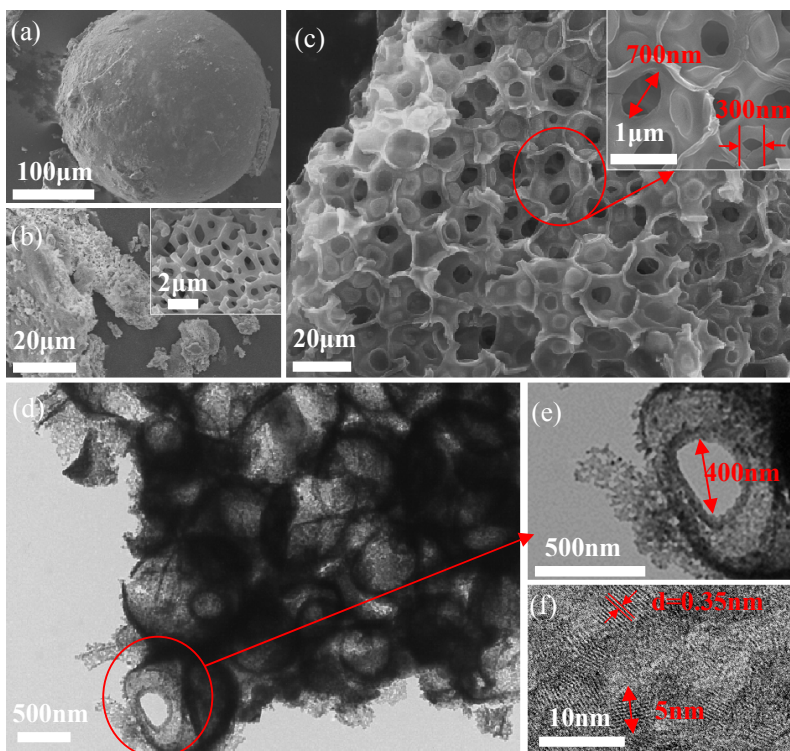


Figure 2. SEM image of (a) Artemia cyst shell, (b) AS debris (after ball milling), (c) the as-prepared hierarchical porous TiO₂; (d) TEM image of the as-prepared hierarchical porous TiO₂; (e) the corresponding local magnified image of (d); (f) the corresponding HRTEM image

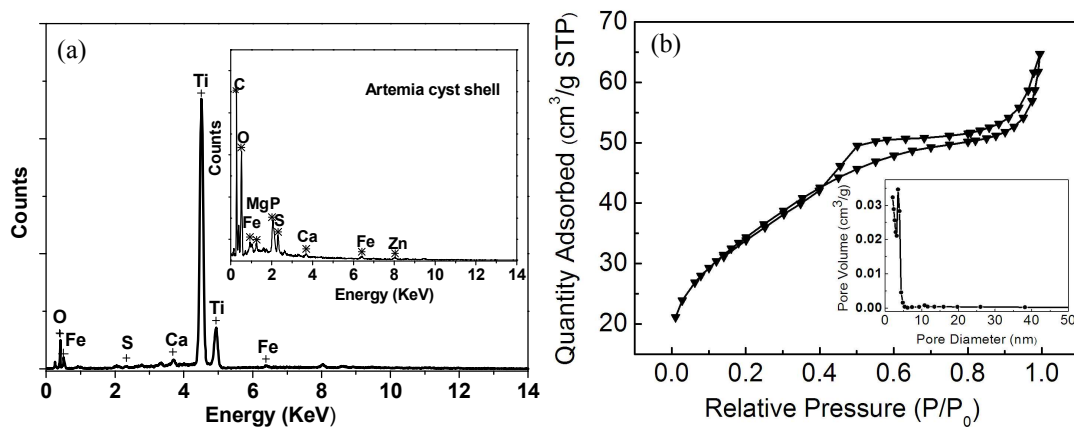


Figure 3. (a) EDS patterns of the as-prepared TiO_2 and template AS (inset); (b) Nitrogen adsorption-desorption isotherms plots and pore size distribution plots of as-prepared TiO_2 (inset).

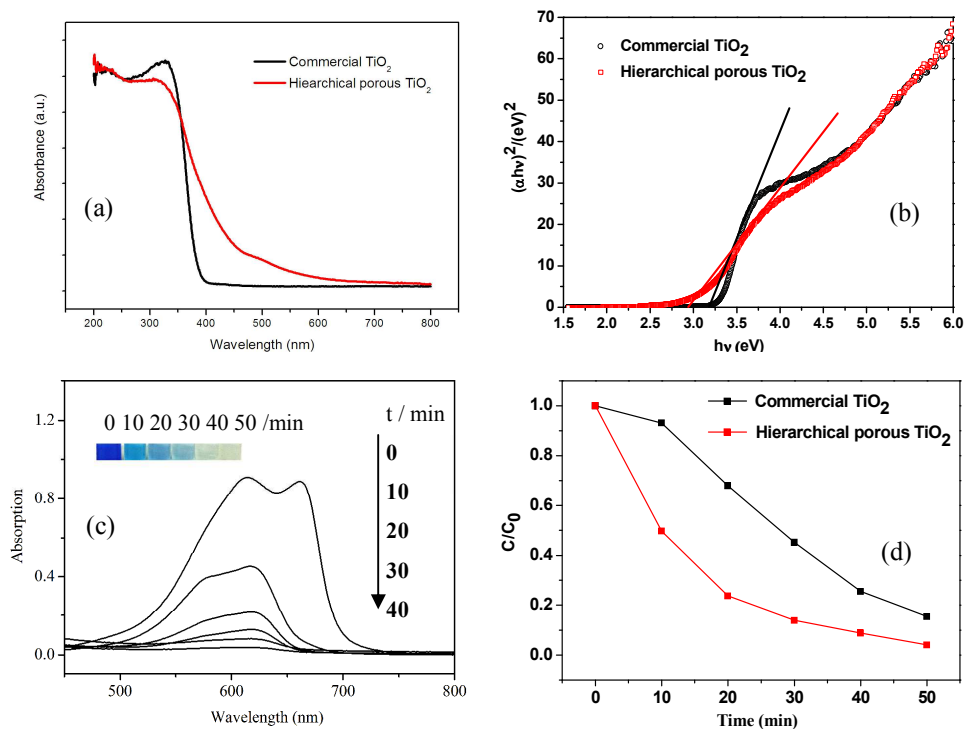


Figure 4. (a) UV-Visible absorption spectrum; (b) plot of $(\alpha h\nu)^2$ versus $h\nu$ for the TiO₂ samples; (c) Time-dependent color change and corresponding time-dependent absorption spectrum of MB in the presence of as-prepared TiO₂; (d) the degree of MB degradation with catalysts versus the exposure time, where C_0 refers to the initial methylene blue concentration (after the dark reaction).

A novel hierarchical porous TiO_2 is synthesized using a natural *Artemia* cyst shell as template, showing improved photocatalytic performance.

